Nuclear Instruments and Methods in Physics Research B 352 (2015) 18–21

Contents lists available at ScienceDirect

Nuclear Instruments and Methods in Physics Research B

journal homepage: www.elsevier.com/locate/nimb

A hybrid model describing ion induced kinetic electron emission

S. Hanke *, A. Duvenbeck, C. Heuser, B. Weidtmann, A. Wucher

Fakultät für Physik, Universität Duisburg-Essen, 47048 Duisburg, Germany

ARTICLE INFO

Article history:
Received 11 July 2014
Received in revised form 23 December 2014
Accepted 8 January 2015
Available online 10 February 2015

Keywords:
Hybrid model
Richardson–Dushman
Impact angle dependence
Electron emission yield
Molecular dynamics

ABSTRACT

We present a model to describe the kinetic internal and external electron emission from an ion bombarded metal target. The model is based upon a molecular dynamics treatment of the nuclear degree of freedom, the electronic system is assumed as a quasi-free electron gas characterized by its Fermi energy, electron temperature and a characteristic attenuation length.

In a series of previous works we have employed this model, which includes the local kinetic excitation as well as the rapid spread of the generated excitation energy, in order to calculate internal and external electron emission yields within the framework of a Richardson–Dushman-like thermionic emission model. However, this kind of treatment turned out to fail in the realistic prediction of experimentally measured internal electron yields mainly due to the restriction of the treatment of electronic transport to a diffusive manner. Here, we propose a slightly modified approach additionally incorporating the contribution of hot electrons which are generated in the bulk material and undergo ballistic transport towards the emitting interface.

1. Introduction

The bombardment of solid metal surfaces with keV ions leads to the emission of particles from the surface [1,2]. It is well known that the nuclear particle kinetics triggered by the projectile impact are accompanied by kinetically induced electronic excitations which manifest in the emission of free electrons (KEE) [3–14]. Recently, excitations below the vacuum level have also been observed in form of an internal electron current across a buried tunneling barrier in ion bombarded metal-insulator-metal (MIM) junctions [15,16]. An experimental observable in this context is the electron emission yield γ, defined as the number of emitted electrons per impinging projectile atoms. In the following, the yields of electrons emitted into the vacuum or transmitted across the tunneling barrier will be referred to as "external" (γ_{ext}) and "internal" (γ_{int}) yields, respectively. Both quantities have been shown to vary as a function of the polar angle of incidence of the projectile in a characteristic fashion, with γ_{ext} increasing and γ_{int} decreasing under increasingly oblique incidence [17,18].

We have recently developed a hot spot model describing the external electron yield in terms of thermionic emission from a locally heated surface. The model treats the electronic system as a quasi-free electron gas which is excited by electronic stopping of all moving particles in the collision cascade. Transport of excitation away from the point of its generation is treated in terms of a diffusive approach, and the resulting excitation energy density profile is parametrized in terms of a locally and temporarily elevated electron temperature. The emission yield is then calculated by means of a modified Richardson–Dushman equation [19]. While this model reproduces measured *external* yields quite well, it fails to explain the observed *internal* yields by orders of magnitude [20]. Analysis shows that this is due to the strongly inhomogenous excitation profile, which exhibits a significantly reduced electron temperature at the tunneling barrier located at a depth of several nm below the surface. In this work, we present a modification of the Richardson–Dushman model in order to include the contribution of hot electrons generated in the bulk volume of the bombarded material to the observed emission yield. In particular, one might expect that electrons produced in the hot near-surface region may be ballistically transported towards the buried interface and contribute to the observed internal emission yield. We will show that such a hybrid model is capable of describing both internal and external yields quite well, but still generates problems regarding the predicted projectile impact angle dependence. In this context, the possible role of anisotropic effects on the excitation and transport processes is discussed.

2. Methods

For the model system of a keV projectile impinging onto a silver surface, we use classical molecular dynamics (MD) to follow the motion of the target atoms and the projectile [21,22]. Briefly, the

* Corresponding author.

http://dx.doi.org/10.1016/j.nimb.2015.01.008
0168-583X/

coupled Newtonian equations of motion are integrated numerically employing a MD/MC-CEM many body potential to describe the interaction among the atoms [23]. Kinetic excitation is incorporated into the model via an electronic friction term entering the equations of motion. Thus, each particle moving with a kinetic energy E_{kin} constitutes a time- and space-dependent source of excitation energy, thereby feeding an energy

$$dE = A \cdot E_{kin} \cdot dt$$

into the electronic system, where the constant A is taken from the Lindhard–Scharff theory [24]. In addition to the electronic friction mechanism, hot electrons may be generated in violent collisions among two atoms [25] via the promotion of inner shell states to energies above the Fermi level. For a more detailed description, the reader is referred to [26].

Depending on the nature of the solid, the excitation energy generated this way will rapidly spread away from the point of its generation. This transport is treated as a heat conduction process via a formal diffusion equation

$$\frac{\partial E(\vec{r},t)}{\partial t} - D\Delta E(\vec{r},t) = \frac{dS(\vec{r},t)}{dt}, \tag{1}$$

where $S(\vec{r},t)$ comprises the excitation source terms and D denotes a diffusivity coefficient which for the present case of an amorphous crystal was chosen as $D = 1\ \mathrm{cm}^2/\mathrm{s}$ [27].

Eq. (1) is numerically solved on a sub-fs timescale using pseudo-infinite boundary conditions as described in detail elsewhere [28]. The resulting excitation energy density is converted into an electron temperature profile $T_e(\vec{r},t)$, which can then be used as input for the thermionic electron emission model.

The scheme underlying the calculation of electron yields is depicted in Fig. 1: Following the standard procedure described by Baragiola et al. [8], we calculate the electron emission arising from a heated layer of thickness Δz located at depth z_i below the surface in the framework of the Richardson–Dushman approach using the corresponding $T_e(\vec{r},t)$ as [19]

$$\gamma_{RD} = \frac{1}{e}\int_0^\infty \int_A j_{RD}(\vec{r},t)\,dA\,dt, \tag{2}$$

with

$$j_{RD}(\vec{r},t) = \frac{em}{2\pi^2\hbar^3}(k_B T_e(\vec{r},t))^2 \times \sum_{n=1}^{\infty}(-1)^{n-1}\frac{1}{n^2}e^{-n\Phi/k_B T_e(\vec{r},t)}, \tag{3}$$

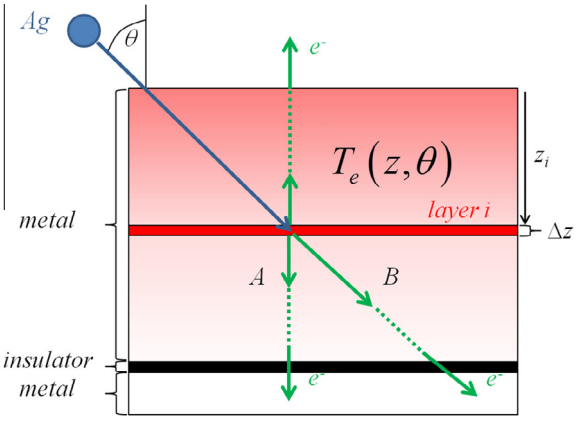

Fig. 1. Schematic view of kinetic electron emission from an ion bombarded metal-insulator-metal target. Kinetic excitation leads to an elevated electron temperature $T_e(z,\theta)$ in the highlighted layer z_i (red). Hot electrons emitted from this heated layer are ballistically transported towards the surface and the buried oxide interface (green arrows), where they contribute to the total external and internal electron emission yield, respectively. For the case of an anisotropic excitation profile, the travel path can be prolonged as indicated by the dashed green line labeled "B". (For interpretation of the references to color in this figure legend, the reader is referred to the web version of this article.)

where the integration is performed over all volume elements (here: cells of 3 Å × 3 Å × 3 Å) belonging to this specific layer. In order to contribute to the (external or internal) emission yield, the hot electrons liberated this way must travel to the surface or the buried interface, respectively, in a ballistic fashion. The probability for this ballistic transport is described by an effective attenuation length λ. In order to calculate the total emission yield, we therefore weigh the contribution of each layer by an exponential attenuation factor and calculate the resulting total external and internal emission yield as

$$\gamma_{hybrid}^{ext} = \sum_i \gamma_{RD} \cdot \exp\left(-\frac{z_i}{\lambda}\right). \tag{4}$$

and

$$\gamma_{hybrid}^{int} = \sum_i \gamma_{RD} \cdot \exp\left(-\frac{d-z_i}{\lambda}\right). \tag{5}$$

The empirical parameter λ can in principle be determined from experimental data. For silver bombarded with Ar^+ ions, the measured exponential dependence of the internal yield on the thickness d of the top metal film indicates an effective attenuation length of about 10 nm [29], which was used in the present calculations. It should be noted that a fundamental assumption underlying Eqs. (4) and (5) is that the excitation is isotropic with respect to the direction of motion of the hot electrons. As indicated below, we have reason to believe that this assumption might be too crude, since each moving particle must also transfer momentum to the electronic system. Since the entire dynamics are triggered by the impinging projectile, the k-distribution of the kinetically generated hot electrons must to some extent be anisotropic and carry a memory of the original direction of the projectile motion. In principle, the largest energy transfer in direct atom-electron collisions underlying the electronic friction picture occurs along the direction of motion of the moving atom. Therefore, one might expect a preferred excitation along the original direction of motion of the impinging projectile. As a consequence, the effective ballistic transport length might be altered as a function of the projectile impact angle as indicated in Fig. 1. In order to obtain a rough estimate of the possible influence of such an effect, one can assume that *all* excited electrons are moving exclusively in that direction, leading to an effective path length of $(d-z_i)/\cos(\theta)$ for the internal yield contribution generated by a projectile impinging under an angle θ with respect to the surface normal.

It should be noted that the model described above constitutes a hybrid approach regarding the transport of excitation within the solid. On one hand, the excitation profile generated by the particle kinetics is calculated via a diffusive (heat conduction) approach, which assumes electron–electron interaction with a rather short mean free path. Along with the assumption of a quasi-thermal excitation energy distribution, we assume this to be valid for the low energy excitations which carry the vast majority of the total excitation energy. The emission yield, on the other hand, is based on the few hot electrons which carry excitation energies above the respective emission thresholds. In line with nearly all existing models describing KEE, Photoelectron or Auger electron emission from a solid surface [8], we assume that these electrons undergo ballistic transport with effective attenuation lengths of the same order as used here.

3. Results

Basis of our calculations is an amorphous silver crystal of 75 Å × 75 Å × 75 Å bombarded with 5-keV Ag atoms under varying polar angle of incidence. By choosing an amorphous target, we avoid the influence of the azimuthal angle of incidence for

non-perpendicular impact of the projectile. To ensure sufficient statistics, a set of 169 impact points is placed equidistantly within a 7 Å × 7 Å square on top of the crystal surface. The chosen size of the model crystal constitutes a reasonable compromise which allows comparison with experimental data at adequate computational time.

Using Eqs. (2), (4) and (5), we calculated the electron emission yields for the Richardson–Dushman and the hybrid model, with $\Phi_B = 3.9$ eV [29] for the internal and $\Phi_W = 4.74$ eV [30] for the external emission yield, respectively. The results are displayed in Fig. 2 as blue (Richardson–Dushman) and red (hybrid model) symbols. For comparison, measurements obtained for 5-keV Ar^+ bombardment of an Ag|AlOx|Al MIM system with a top layer thickness $d_{Ag} = 40$ nm are shown in Fig. 2 as black points (data taken from [31,32]).

The external electron emission yield calculated using the pure Richardson–Dushman approach (blue solid rhombs) increases from 0.3 for normal incidence to 1.9 for $\theta = 80°$. A similar trend is observed for the experimental data (black solid squares), which increase from 0.2 (normal incidence) to 1.2 ($\theta = 80°$). This impact angle dependence of the external electron emission yield is well known in the literature [18], where a $1/\cos(\theta)$-dependence has been established.

The internal electron emission shows a rather different behavior: concentrating on normal incidence, the huge discrepancy of approximately seven orders of magnitude between the calculated internal electron emission yield ($6 \cdot 10^{-8}$, blue hollow rhombs) and the corresponding experimental data (0.16, black hollow squares) as well as the calculated external yield is obvious. Although the experimental data were taken for slightly different bombarding conditions, a difference of more than two orders of magnitude to the calculated value is surprisingly high. In principle, another reason for the deviating results may be the different silver layer thickness. While for the simulations a model crystal of 75 Å is used, the experiments were performed for a top layer thickness of 400 Å. From the work of Meyer et al. [29] it is known that a decrease of layer thickness leads to an exponential increase of the resulting internal electron emission yields. Therefore the calculated yields should be expected to be *above* instead of several orders of magnitude below the measured ones. A possible explanation for this unexpected behavior could be the different penetration depths for the different projectiles, which can be determined using SRIM[1]: for 5-keV Ar atoms bombarding a silver solid a depth of 41 Å is estimated while for 5-keV Ag atoms impinging onto a silver crystal this depth is only 29 Å. Therefore a lower penetration depth for silver projectiles could result in a decrease of the internal electron emission yield since the electrons excited by the Ar-projectiles are generated closer to the buried interface. In addition to the absolute values of the internal emission yields, the impact angle dependence is striking as well. While the experimental data decrease by a factor of three between normal and oblique incidence, the calculated data decrease by 14 orders of magnitude. This decline combined with the huge discrepancy in the absolute values between experimental and calculated data show that the purely diffusive treatment of the transport of electronic excitation is inadequate to describe the processes underlying the internal electron emission.

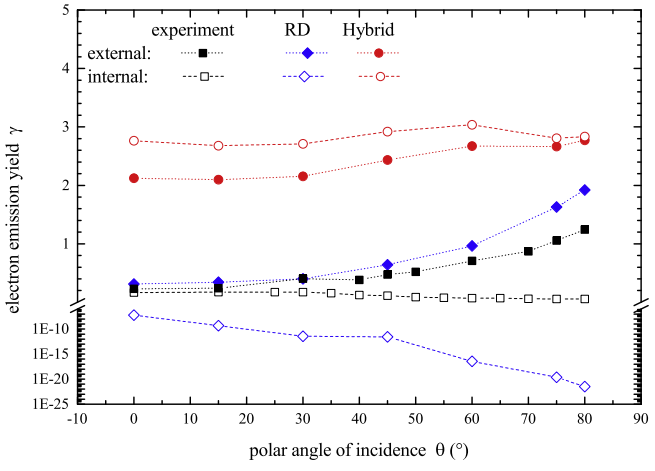

Fig. 2. Electron emission yields as a function of the impact angle, calculated via Richardson–Dushman (blue rhombs) as well as hybrid model (red circles). The data for external emission is characterised by solid symbols, the internal emission yields by hollow ones. Experimental data taken from [31,32]. (For interpretation of the references to color in this figure legend, the reader is referred to the web version of this article.)

As mentioned above, only the electron emission yields resulting from electronic excitations at the top (for the external case) and the bottom (for the internal case) of the model crystal are taken into account within the frame of the pure Richardson–Dushman-formalism. Fig. 2 also shows the calculated data for the hybrid model (red circles), which incorporates the ballistic transport of the electronic excitations generated in deeper layers in the crystal. These additional contributions lead to an increase of both the external as well as the internal electron emission yield as is expected from the inclusion of additional contributions. While the increase of the external yield (factor 6) is moderate, the main advantage of the hybrid model is related to the prediction of the internal yield. As seen from Fig. 2, this value is now substantially increased and becomes comparable with the external yield, as measured experimentally. This finding represents clear indication that ballistic transport of the excited electrons must play an important role in determining this yield.

However, no significant angular dependence is observed in the calculations, indicating that there is still a problem with the model. In order to tackle this problem, we implement a possible way to include an anisotropic excitation into the calculations described in Section 2. In principle, one should calculate the excitation profile as done, for instance, in Ref. [33]. However, such calculations are too complex to be incorporated in our model. In order to still elucidate the influence on the kinetic electron emission process, we use a first order approximation as indicated in Fig. 1 and assume that all relevant excited electrons move along the original direction of motion of the impinging projectile. This assumption may be seen as an upper estimation for the influence of the excitation anisotropy on the electron emission yield. The resulting impact angle dependence of the predicted internal yield is presented in Fig. 3.

It is seen that the model now qualitatively predicts the correct impact angle dependence, although the decrease towards oblique incidence is too pronounced, indicating that the assumption of exclusively directional excitation is too coarse. This is understandable, since about 50% of the total excitation energy is contributed by the recoils [34] which move in rapidly randomized directions.

4. Conclusion

While the pure Richardson–Dushman formalism only reproduces the observed kinetic external electron emission yield, the improved hybrid model is capable to predict emission yields of the same order of magnitude for both the external and the internal emission process. The results presented here indicate that each layer of an ion bombarded solid acts as a thermal emitter of hot electrons that are ballistically transported to the relevant emitting

[1] www.SRIM.org.

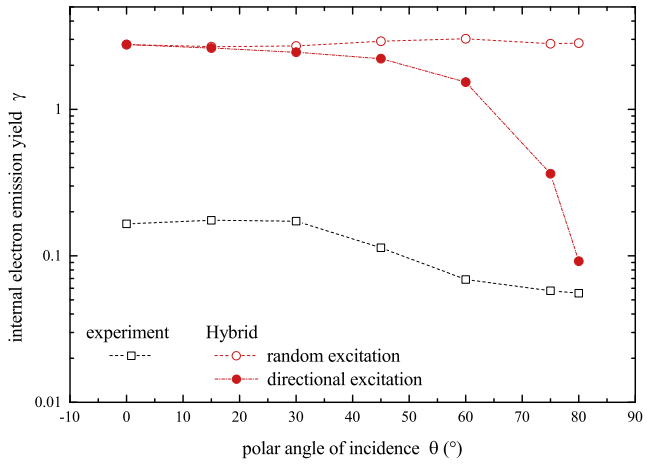

Fig. 3. Internal electron emission yields as a function of the polar angle of incidence for directional (red solid circles) and random excitation (red hollow circles). Experimental data taken from [31]. (For interpretation of the references to color in this figure legend, the reader is referred to the web version of this article.)

surface. With regard to the directional excitation of the hot electrons created by the projectile, the observed impact angle dependence of the internal emission yield can be qualitatively reproduced, although the decrease is overestimated.

In principle, a more sophisticated description of the electronic transport can be achieved by numerically solving the corresponding Boltzmann transport equation (BTE). The explicit computations, however, turn out to be far too complex and computer time expensive to allow for a comprehensive treatment of kinetic electron emission phenomena. Nevertheless, exemplary model calculations within the framework of the BTE can be used to extract physical parameters – such as the diffusivity D – that enter the model presented here. Corresponding calculations are currently under way in our lab.

Acknowledgement

We acknowledge financial support from the Deutsche Forschungsgemeinschaft within the frame work of the SFB 616 “Energy Dissipation at Surfaces”. We would also like to thank B.J. Garrison for providing us with the amorphous model crystal.

References

[1] P. Sigmund, Sputtering by ion bombardment theoretical concepts, in: R. Behrisch (Ed.), Sputtering by Particle Bombardment I, Topics Applied Physics, vol. 47, Springer, Berlin Heidelberg, 1981, pp. 9–71.
[2] Z. Sroubek, X. Chen, J.A. Yarmoff, Phys. Rev. B 73 (2006) 045427.
[3] E.V. Alonso, R.A. Baragiola, J. Ferrón, M.M. Jakas, A. Oliva-Florio, Phys. Rev. B 22 (1) (1980) 80–87.
[4] E.V. Alonso, M.A. Alurralde, R.A. Baragiola, Surf. Sci. 166 (2–3) (1986) L155–L160.
[5] R.A. Baragiola, E.V. Alonso, A.O. Florio, Phys. Rev. B 19 (1979) 121–129.
[6] R.A. Baragiola, E.V. Alonso, J. Ferron, A. Oliva-Florio, Surf. Sci. 90 (2) (1979) 240–255.
[7] R.A. Baragiola, E.V. Alonso, A. Oliva, A. Bonnano, F. Xu, Phys. Rev. A 45 (7, B) (1992) 5286–5288.
[8] R.A. Baragiola, Nucl. Instr. Meth. B 78 (1993) 223–238.
[9] M. Commisso, M. Minniti, A. Sindona, A. Bonanno, A. Oliva, R.A. Baragiola, P. Riccardi, Nucl. Instr. Meth. B 256 (1) (2007) 474–477.
[10] H. Eder, W. Messerschmidt, H. Winter, F. Aumayr, J. Appl. Phys. 87 (11) (2000) 8198–8200.
[11] J. Ferrón, E.V. Alonso, R.A. Baragiola, A. Oliva-Florio, J. Phys. D: Appl. Phys. 14 (9) (1981) 1707–1719.
[12] A. Oliva-Florio, R.A. Baragiola, M.M. Jakas, E.V. Alonso, J. Ferrón, Phys. Rev. B 35 (5) (1987) 2198–2204.
[13] K. Töglhofer, F. Aumayr, H.P. Winter, Surf. Sci. 281 (1–2) (1993) 143–152.
[14] H. Winter, H. Eder, F. Aumayr, J. Lorincik, Z. Sroubek, Nucl. Instr. Meth. B 182 (2001) 15–22.
[15] D. Diesing, G. Kritzler, M. Stermann, D. Nolting, A. Otto, J. Solid State Electr. 7 (2003) 389–415.
[16] S. Meyer, D. Diesing, A. Wucher, Phys. Rev. Lett. 93 (2004) 137601.
[17] C. Heuser, M. Marpe, D. Diesing, A. Wucher, Nucl. Instr. Meth. B 267 (2009) 601–604.
[18] J. Ferron, E. Alonso, R. Baragiola, A. Olivaflorio, Phys. Rev. B 24 (1981) 4412–4419.
[19] D.A. Kovacs, T. Peters, C. Haake, M. Schleberger, A. Wucher, A. Golczewski, F. Aumayr, D. Diesing, Phys. Rev. B 77 (2008) 245432.
[20] S. Hanke, A. Duvenbeck, C. Heuser, B. Weidtmann, D. Diesing, M. Marpe, A. Wucher, Nucl. Instr. Meth. B 303 (2013) 55–58.
[21] H.M. Urbassek, Nucl. Instr. Meth. B 122 (1997) 427–441.
[22] D. Harrison, P.W. Kelly, B. Garrison, N. Winograd, Surf. Sci. 76 (1978) 311–322.
[23] C. Kelchner, D. Halstead, L. Perkins, N.W.A. DePristo, Surf. Sci. 310 (1994) 425.
[24] J. Lindhard, M. Scharff, Phys. Rev. 124 (1961) 128.
[25] U. Fano, W. Lichten, Phys. Rev. B 14 (1965) 627.
[26] A. Duvenbeck, B. Weidtmann, O. Weingart, A. Wucher, Phys. Rev. B 77 (2008) 245444.
[27] B. Weidtmann, S. Hanke, A. Duvenbeck, A. Wucher, Surf. Interface Anal. 43 (2011) 24–27.
[28] A. Duvenbeck, A. Wucher, Phys. Rev. B 72 (2005) 165408.
[29] S. Meyer, C. Heuser, D. Diesing, A. Wucher, Phys. Rev. B 78 (2008) 035428.
[30] H.B. Michaelson, J. Appl. Phys. 48 (1977) 4729–4733.
[31] M. Marpe, C. Heuser, D. Diesing, A. Wucher, Nucl. Instr. Meth. B 269 (2011) 972–976.
[32] C. Heuser, A. Wucher, Nucl. Instr. Meth. B 317 (2013) 37–43.
[33] J. Juaristi, M. Rösler, F. García de Abajo, Phys. Rev. B 58 (1998) 15838–15846.
[34] A. Duvenbeck, O. Weingart, V. Buss, A. Wucher, Nucl. Instr. Meth. B 258 (2007) 83–86.